

Article

# Controlling the Redox Catalytic Activity of a Cyclic Selenide Fused to 18-Crown-6 by the Conformational Transition Induced by Coordination to an Alkali Metal Ion

Michio Iwaoka<sup>1,2,\*</sup> , Hajime Oba<sup>1</sup> and Takeru Ito<sup>1</sup> 

<sup>1</sup> Department of Chemistry, School of Science, Tokai University, Hiratsuka-shi 259-1292, Kanagawa, Japan; 7bsc1112@gmail.com (H.O.); takeito@keyaki.cc.u-tokai.ac.jp (T.I.)

<sup>2</sup> Institute of Advanced Biosciences, Tokai University, Hiratsuka-shi 259-1292, Kanagawa, Japan

\* Correspondence: miwaoka@tokai.ac.jp; Tel.: +81-463-63-4356

**Abstract:** *trans*-3,4-Dihydroxyselenolane (DHS), a water-soluble cyclic selenide, exhibits selenoenzyme-like unique redox activities through reversible oxidation to the corresponding selenoxide. Previously, we demonstrated that DHS can be applied as an antioxidant against lipid peroxidation and a radioprotector by means of adequate modifications of the two hydroxy (OH) groups. Herein, we synthesized new DHS derivatives with a crown-ether ring fused to the OH groups (DHS-crown-*n* (*n* = 4 to 7), 1–4) and investigated their behaviors of complex formation with various alkali metal salts. According to the X-ray structure analysis, it was found that the two oxygen atoms of DHS change the directions from diaxial to diequatorial by complexation. The similar conformational transition was also observed in solution NMR experiments. The <sup>1</sup>H NMR titration in CD<sub>3</sub>OD further confirmed that DHS-crown-6 (**3**) forms stable 1:1 complexes with KI, RbCl and CsCl, while it forms a 2:1 complex with KBPh<sub>4</sub>. The results suggested that the 1:1 complex (**3**·MX) exchanges the metal ion with metal-free **3** through the formation of the 2:1 complex. The redox catalytic activity of **3** was evaluated using a selenoenzyme model reaction between H<sub>2</sub>O<sub>2</sub> and dithiothreitol. The activity was significantly reduced in the presence of KCl due to the complex formation. Thus, the redox catalytic activity of DHS could be controlled by the conformational transition induced by coordination to an alkali metal ion.

**Keywords:** selenide; crown ethers; coordination chemistry; conformational analysis; NMR titration; redox catalysis; enzyme mimics; ion sensors



**Citation:** Iwaoka, M.; Oba, H.; Ito, T. Controlling the Redox Catalytic Activity of a Cyclic Selenide Fused to 18-Crown-6 by the Conformational Transition Induced by Coordination to an Alkali Metal Ion. *Molecules* **2023**, *28*, 3607. <https://doi.org/10.3390/molecules28083607>

Academic Editor: Francesca Marini

Received: 29 March 2023

Revised: 18 April 2023

Accepted: 18 April 2023

Published: 20 April 2023



**Copyright:** © 2023 by the authors. Licensee MDPI, Basel, Switzerland. This article is an open access article distributed under the terms and conditions of the Creative Commons Attribution (CC BY) license (<https://creativecommons.org/licenses/by/4.0/>).

## 1. Introduction

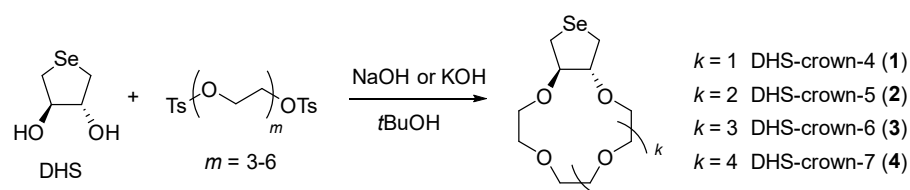
Crown ethers have been widely utilized as synthetic modules for various functional molecules because they can selectively accommodate a metal ion in the cavity or a polymer chain through the hole [1,2]. In particular, the molecular recognition functions of crown ethers are essential in designing rotaxane-based molecular machines [3–5] and molecular sensors [6–9]. Since the discovery, crown ethers and their analogues that involve chalcogen atoms, i.e., S, Se and Te, instead of the oxygen atoms [1,10,11] have been elaborately studied from various points of view. For example, thia-crown ethers have been employed as extractants for heavy metal ions [12–15]. Redox responses as well as catalytic functions of some thia- and seleno-crown ethers were investigated [16–21]. Molecular assemblies through chalcogen bonding interactions have also been studied recently for telluro-ether heterocycles [22].

*trans*-3,4-Dihydroxyselenolane (DHS) is a water-soluble five-membered ring selenide with a selenoenzyme-like unique redox catalytic activity through the reversible oxidation to the selenoxide >Se=O (DHS<sup>ox</sup>) [23,24]. It is also a stable molecule with low toxicity [25,26]. These features are potential merits of DHS when it is applied to medicinal and material

sciences. We previously demonstrated that DHS can be an antioxidant against lipid peroxidation [27,28] and a radioprotector [29] by means of adequate chemical modifications of the two hydroxy (OH) groups. In this study, we developed new DHS derivatives with a crown-ether ring fused to the OH groups (DHS-crown- $n$  ( $n = 4$  to 7), 1–4) and investigated their behaviors as host molecules to various alkali metal salts. Moreover, the redox catalytic activity of one of the new DHS derivatives, i.e., DHS-crown-6 (3), was evaluated in a selenoenzyme model reaction. It was found that the activity can be controlled by the complexation with a potassium ion ( $K^+$ ).

## 2. Results and Discussion

DHS-crowns (1–4) were synthesized in the yields of 40 to 59% by the coupling reaction between DHS and the corresponding ditosylates in the presence of NaOH or KOH as a template (Scheme 1). The obtained compounds were characterized by  $^1H$ ,  $^{13}C$  and  $^{77}Se$  NMR as well as MS spectrometry.



**Scheme 1.** Synthesis of DHS-crown- $n$  ( $n = 4$  to 7).

The molecular structure of DHS-crown-4 (1) was determined by X-ray analysis (Figure 1). The two oxygen atoms of DHS fused by the 12-crown-4 ring occupied axial positions of the five-membered ring of DHS. Similar diaxial conformations are commonly observed for the parent DHS [30] and its derivatives [31,32]. This is probably due to the electrostatic repulsion between the two negatively charged oxygen atoms.

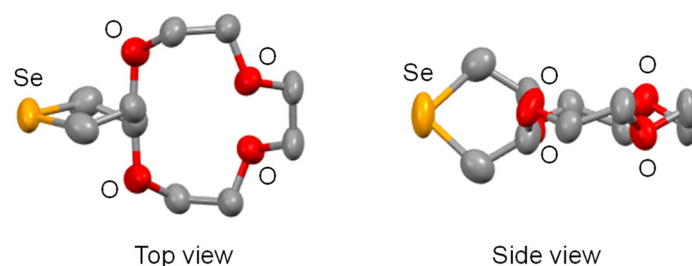


**Figure 1.** X-ray structure for DHS-crown-4 (1). Ellipsoids are drawn with 50% probabilities.

We subsequently investigated the complex formation of 1–4 with an alkali metal ion. Fine single crystals were obtained when the host molecules 1–3 were mixed in methanol with KI or NaBr as a salt. Figure 2 shows the molecular structures for 1·0.5KI·H<sub>2</sub>O (5), 1·0.5NaBr·2H<sub>2</sub>O (6), 2·0.5KI (7) and 3·KI (8).

For DHS-crown-4 (1), 2:1 complexes (5 and 6) with KI and NaBr, respectively, were crystallized. Complex 5 showed a distorted sandwich-type shape owing to the smaller cavity of 12-crown-4, which pushed the larger alkali ion ( $K^+$ ) out of the cavity. The position of the counter anion ( $I^-$ ) was close to  $K^+$  ( $r_{K...I} = 3.537(1)$  Å). This weak coordination interaction enforced the two crown-ether rings open in one side. On the other hand, in complex 6, the counter anion ( $Br^-$ ) did not have an interaction with  $Na^+$ , allowing for the two crown-ether rings in an almost parallel configuration. This would be because  $Na^+$  can enter the cavity of the 12-crown-4 ring deeper than  $K^+$  due to the smaller ion radius.

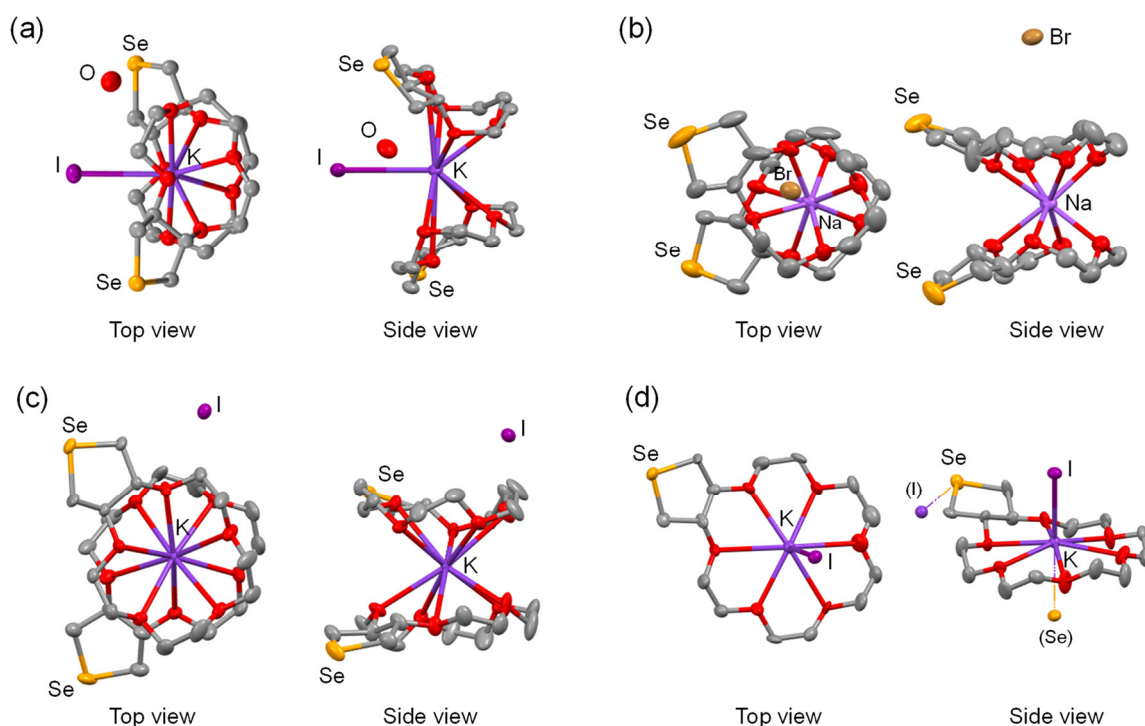


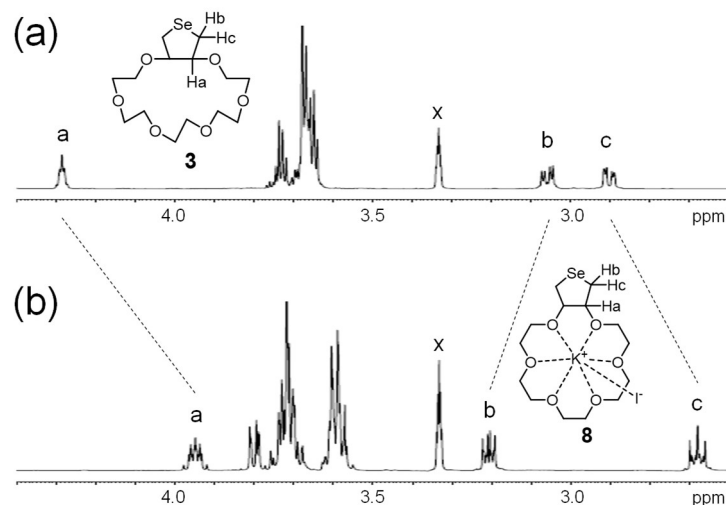
**Figure 2.** X-ray structures for the alkali metal complexes of DHS-crown-*n*. (a) DHS-crown-4 (1)·0.5KI·H<sub>2</sub>O (5). (b) DHS-crown-4 (1)·0.5NaBr·2H<sub>2</sub>O (6) with water molecules omitted for clarity. (c) DHS-crown-5 (2)·0.5KI (7). (d) DHS-crown-6 (3)·KI (8). Ellipsoids are drawn with 50% probabilities.

A similar parallel sandwich-type structure to complex 6 was observed for complex 7, in which K<sup>+</sup> entered the cavity of the 15-crown-5 ring of 2 a little more deeply than in the case of complex 5. On the other hand, in complex 8, K<sup>+</sup> resided in the center of the 18-crown-6 ring of 3, forming a flat 1:1 complex. In this complex, the counter anion (I<sup>-</sup>) existed close to K<sup>+</sup> ( $r_{K...I} = 3.413(2)$  Å), blocking one apical site of K<sup>+</sup>, and the other apical site was occupied by the Se atom of the other DHS-crown-6 molecule (3), forming a weak Se···K<sup>+</sup> interaction ( $r_{K...Se} = 3.398(2)$  Å). By comparing the structure of 8 with those of complexes 5 and 7, it is seen that K<sup>+</sup> was captured by the crown-ether ring more strongly with an increasing ring size.

It is notable that, in all complexes (5–8), the two oxygen atoms of DHS occupied the equatorial directions. This contrasts with the observation that the oxygen atoms occupied the axial directions in the metal-free form of DHS-crown-4 (1) (Figure 1). The conformational transition can be reasonably explained by considering that the two oxygen atoms in the axial positions are too far apart from each other to coordinate to a metal ion. Thus, the DHS ring of DHS-crowns would change the conformation from diaxial to diequatorial by complex formation with an alkali metal ion.

Subsequently, the complexation process of DHS-crown-6 (3) was investigated in more detail by NMR to confirm the axial to equatorial conformational transition observed in the solid state. The <sup>1</sup>H NMR spectrum for 3 in CD<sub>3</sub>OD (Figure 3a) showed the signal for the H<sub>a</sub> proton of the DHS ring at 4.29 ppm as multiplet, while those for the H<sub>b</sub> and H<sub>c</sub> protons at 3.06 and 2.90 ppm were shown as doublet of doublets. These spectral features were almost identical with those observed in the <sup>1</sup>H NMR spectra for the other DHS-crowns, i.e., 1, 2 and 4, suggesting that the metal-free forms of 1–4 maintain the same conformation in the solution. However, when KI (1 eq) was added, significant changes in the NMR spectrum were observed (Figure 3b). The signal for H<sub>a</sub> shifted upfield from 4.29 to 3.95 ppm, and the signals for the CH<sub>2</sub> protons appeared as largely separated peaks at 3.21 and 2.68 ppm. The profiles of the peaks also became different from those observed before the addition of KI. The spectral changes strongly supported the conformational transition induced by

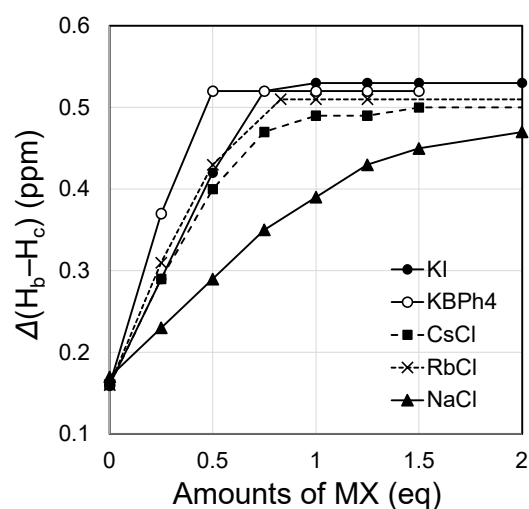
coordination to  $K^+$ . Similarly, significant spectral changes were observed in the  $^{13}C$  and  $^{77}Se$  NMR spectra for **3** after the addition of KI (see SI).



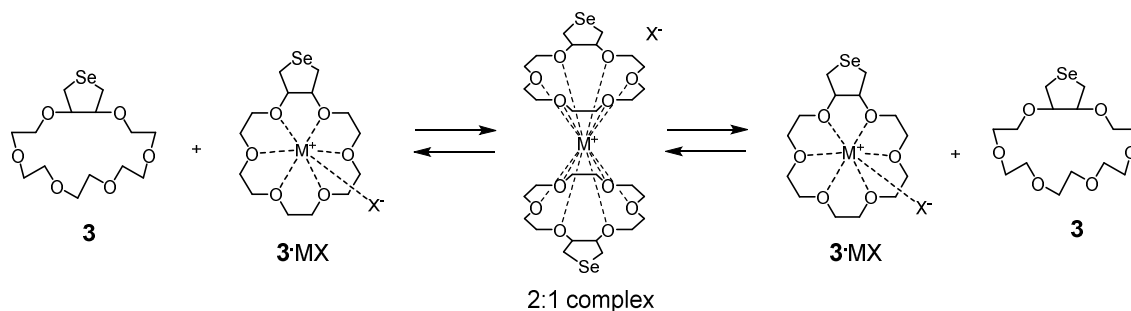
**Figure 3.** 500 MHz  $^1H$  NMR spectra for **3** in  $CD_3OD$ . (a) In the absence of KI. (b) After the addition of 1 eq of KI. “x” indicates the solvent peak.

Figure 4 shows the changes in the peak separation between H<sub>b</sub> and H<sub>c</sub> protons of **3** ( $\Delta(H_b - H_c)$ ) in the  $^1H$  NMR spectrum when a variable amount of an alkali metal salt (MX) was added. The separation width gradually increased with the addition of MX, indicating that the metal ion ( $M^+$ ) was rapidly exchanged among the host molecules within a time scale of the NMR measurement. The observed titration curves clearly show that stable 1:1 complexes were completely produced not only with KI but also with CsCl and RbCl when 1 eq of the metal salts were added, because  $\Delta(H_b - H_c)$  reached plateaus. On the other hand, NaCl seemed to form the 1:1 complex with **3** in equilibrium with the metal-free host, as  $\Delta(H_b - H_c)$  was still increasing when 2 eqs of the salt were added. The formation of the less stable complex would be due to the smaller size of  $Na^+$  compared to the 18-crown-6 cavity of **3**. Interestingly, when potassium tetraphenylborate ( $KBPh_4$ ) was employed as a salt, the peak separation became a maximum with the addition of 0.5 eq, suggesting the formation of a stable 2:1 complex. This complex would have a sandwich-type structure like those observed for complexes **6** and **7** (Figure 2) and should have become stable because the counter anion ( $BPh_4^-$ ) does not possess a coordinating ability. According to these observations, we propose the mechanism for the rapid exchange of an alkali metal ion between DHS-crown-6 molecules (**3**), as illustrated in Figure 5. In this model, the cation exchange is mediated by the formation of a 2:1 complex, which would be stable when a counter anion ( $X^-$ ) is non-coordinating, such as  $BPh_4^-$ , while it would decompose to the 1:1 complex (**3**·MX) and the metal-free host (**3**) when  $X^-$  is a coordinating ligand, such as  $I^-$ . Indeed,  $\Delta(H_b - H_c)$  became saturated before the addition of 1 eq of KI (Figure 4), suggesting the transient formation of the 2:1 complex during the NMR titration.

According to the X-ray and  $^1H$  NMR studies on the complexation process of DHS-crown-6 (**3**), it is now obvious that the conformation of **3** can be controlled by the coordination to an alkali metal ion. We next planned to apply this interesting property to a molecule device, in which the redox catalytic activity of DHS can be turned on or off by the addition of an alkali metal ion. It is well established that DHS can be oxidized to the selenoxide  $>Se=O$  ( $DHS^{ox}$ ) with  $H_2O_2$  and  $DHS^{ox}$  can be easily reduced back to DHS with thiol (RSH) [24]. This reaction cycle has been used as a model enzyme reaction of selenium-dependent glutathione peroxidase (GPx), because  $H_2O_2$ , a representative reactive oxygen species, is catalytically degraded to  $H_2O$ . Therefore, the similar redox behaviors were expected for DHS-crowns.



**Figure 4.** Peak separation widths for  $H_b$  and  $H_c$  protons of **3** [ $\Delta(H_b - H_c)$ ] in the  $^1H$  NMR spectra as a function of the amounts of alkali metal salt MX added. The spectra were measured in  $CD_3OD$ .



**Figure 5.** A plausible mechanism for an alkali metal ion exchange between two molecules of **3**.

Indeed, host molecule **3** exhibited the GPx-like catalytic activity in the reaction between  $H_2O_2$  and dithiothreitol ( $DTT^{red}$ ) (Figure 6, Cycle A). When the reaction was tracked by  $^1H$  NMR in  $CD_3OD$  at room temperature, the disappearance of  $DTT^{red}$  and the formation of the oxidized disulfide ( $DTT^{ox}$ ) were observed with the reaction progression (see SI). The residual amounts of  $DTT^{red}$  as a function of the reaction time are graphically shown in Figure 7. The catalytic activity of **3** was almost equal to that of the parent DHS [24]. On the other hand, when KCl was added to **3**, the activity was significantly reduced. The half-life time of  $DTT^{red}$  ( $t_{1/2}$ ) increased by about fourfold in the presence of KCl ( $t_{1/2} \sim 240$  min vs.  $\sim 60$  min in the absence of KCl). It should be noted that the presence of KCl did not affect the catalytic activity for the DHS and blank, while KI itself exerted a substantial catalytic activity in this reaction system. The reduction in the catalytic activity of **3** would be due to the conformational change induced by coordination to  $K^+$  (Figure 6, Cycle B). Indeed, a strong capture of  $K^+$  by the crown-ether ring during the catalytic cycle was confirmed as follows. When KCl (1 eq) was added to the selenoxide of **3** ( $3^{ox}$ ), which was generated by reacting **3** with  $H_2O_2$  in  $CD_3OD$ , complete spectral changes were observed in  $^1H$  and  $^{77}Se$  NMR, indicating the formation of the stable  $3^{ox} \cdot K^+$  complex. This complex was easily converted to the  $3 \cdot K^+$  complex by the addition of excess  $DTT^{red}$  (see SI).

To rationalize the reason for the reduction in the redox catalytic activity of **3** in the presence of KCl, the density functional theory calculation was carried out at B3LYP/6-311+G(2df,p) with RCM (solvent = MeOH) for the diaxial and diequatorial conformers of DHS. As a result, it was found that the HOMO energy level of the diequatorial conformer ( $-6.15$  eV) is lower than that of the diaxial conformer ( $-6.01$  eV). Since the rate-determining step of the catalytic cycle of DHS is the oxidation process of DHS to  $DHS^{ox}$ , the decrease in the catalytic activity can be reasonably explained by the conformational change in the DHS

ring of **3** from diaxial to diequatorial due to the complexation of the 18-crown-6 ring to the metal ion.

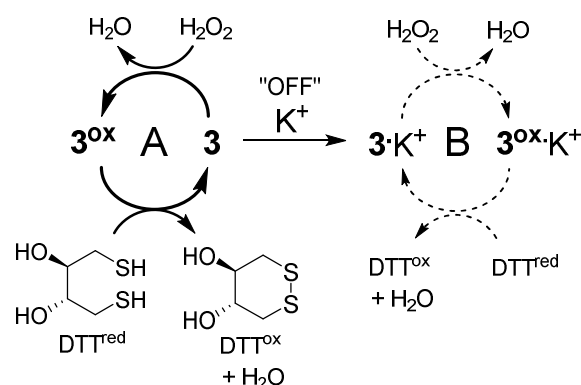


**Figure 6.** Regulation of the redox catalytic activity of DHS-crown-6 (**3**) by the addition of  $K^+$  in the GPx model reaction between  $H_2O_2$  and  $DTT^{red}$ . Cycle A proceeds rapidly, while Cycle B proceeds slowly because of the conformational transition of **3** induced by coordination to  $K^+$ .

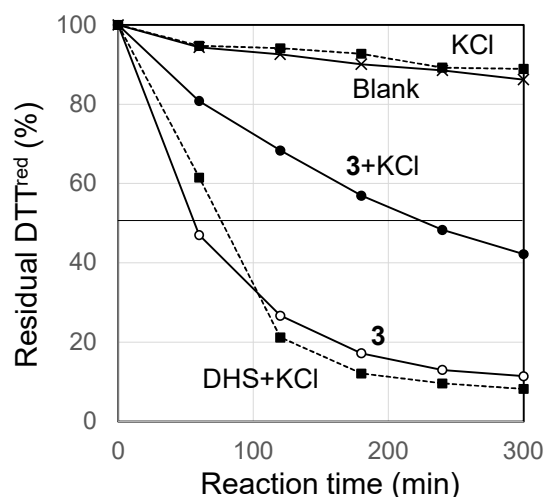


**Figure 7.** Percentages of residual  $DTT^{red}$  as a function of the reaction time in the oxidation of  $DTT^{red}$  with  $H_2O_2$  in the presence of DHS-crown-6 (**3**) in  $CD_3OD$ . Reaction conditions:  $[DTT^{red}]_0 = [H_2O_2]_0 = 0.14$  mol/L and  $[3] = 0.014$  mol/L at  $25^\circ C$  in the absence or presence of KCl (0.014 mol/L).

### 3. Materials and Methods

#### 3.1. General

$^1H$  (500 MHz),  $^{13}C$  (125.8 MHz) and  $^{77}Se$  (95.4 MHz) NMR spectra were recorded on a Bruker AV-500 spectrometer at 298 K in  $CDCl_3$  or  $CD_3OD$ , using the solvent signals as internal standards. For  $^{77}Se$  NMR, dimethyl diselenide was used as an external standard. MALDI-TOF mass spectra were recorded on a JEOL JMS-S3000 mass spectrometer with a high-resolution mode. The sample was dispersed in the matrix of  $\alpha$ -cyano-4-hydroxycinnamic acid (CHCA), with silver nitrate as a cationization agent and polyethylene glycol as an internal standard. All reactions for the synthesis were monitored by thin-layer chromatography (TLC), which was performed on precoated sheets of silica gel 60 purchased from Merck Millipore. Gel permeation chromatography (GPC) was performed with a JAI LC-918 high-performance liquid chromatograph (HPLC) system equipped with JAIGEL-1H/2H preparative columns, using  $CHCl_3$  as an eluent at a flow rate of 3.5 mL/min. No calibration was applied. Racemic *trans*-3,4-dihydroxyselenolane (DHS) was synthesized according to the literature procedure [30,33]. Ditosylates, which were used for the preparation of DHS-crown-*n* (**1–4**), were synthesized according to the literature method, with

slight modifications [34]. All other chemicals were used as purchased without further purification.

### 3.2. Synthesis of 10a,13a-trans-Decahydroselenopheno[3,4-b][1,4,7,10]tetraoxacyclododecine (1)

In a 30 mL round-bottom flask, DHS (52 mg, 0.31 mmol) and KOH (87 mg, 4 eq) were dissolved in *tert*-butyl alcohol (4 mL), and the mixture was stirred at 50 °C for 10 min. To the resulting solution, a solution of triethyleneglycol ditosylate (188 mg, 1.3 eq) in dichloromethane (1 mL) and then *tert*-butyl alcohol (6 mL) was added. The mixture was stirred at 80 °C for 1 h and then refluxed for 20 h. The resulting pale-yellow suspension was added with a saturated aqueous solution of ammonium chloride and extracted with AcOEt ( $\times 3$ ). The combined organic layer was washed with brine and dried over magnesium sulfate. The crude product obtained was purified by GPC to afford DHS-crown-4 (1) as colorless crystals. Yield 35.4 mg (40%). m.p. 42–46 °C. Spectral for 1:  $^1\text{H}$  NMR ( $\text{CDCl}_3$ )  $\delta$  4.34 (m, 2H), 3.72 (m, 4H), 3.66 (m, 4H), 3.53 (m, 4H), 2.96 (dd,  $J = 5.0$  and  $10.0$  Hz, 2H), 2.74 (dd,  $J = 5.0$  and  $10.0$  Hz, 2H).  $^{13}\text{C}$  NMR ( $\text{CDCl}_3$ )  $\delta$  86.2, 72.6, 70.5, 69.2, 24.1.  $^{77}\text{Se}$  NMR ( $\text{CDCl}_3$ )  $\delta$  85.2. HRMS (MALDI-TOF-MS)  $m/z$  calcd for  $\text{C}_{10}\text{H}_{18}\text{AgO}_4\text{Se}^+$   $[\text{M}+\text{Ag}]^+$ : 388.9416. Found: 388.9468. The molecular structure of 1 was determined by X-ray analysis for the crystals recrystallized from methanol (see below).

### 3.3. Synthesis of 13a,16a-trans-Dodecahydroselenopheno[3,4-b][1,4,7,10,13]pentaoxacyclopentadecine (2)

Following a similar procedure, DHS-crown-5 (2) was obtained from DHS (105 mg, 0.63 mmol) and tetraethyleneglycol ditosylate (320 mg, 1.0 eq) as a colorless oil. The crude product was purified by silica gel column chromatography (dichloromethane–methanol 9:1) and GPC. Yield 111 mg (55%). Spectral for 2:  $^1\text{H}$  NMR ( $\text{CDCl}_3$ )  $\delta$  4.39 (m, 2H), 3.81 (m, 2H), 3.73–3.65 (m, 14H), 3.06 (dd,  $J = 3.5$  and  $10.0$  Hz, 2H), 2.91 (br d,  $J = 10.0$  Hz, 2H).  $^{13}\text{C}$  NMR ( $\text{CDCl}_3$ )  $\delta$  85.7, 71.4, 70.6, 70.5, 68.8, 25.1.  $^{77}\text{Se}$  NMR ( $\text{CDCl}_3$ )  $\delta$  93.5. HRMS (MALDI-TOF-MS)  $m/z$  calcd for  $\text{C}_{12}\text{H}_{22}\text{AgO}_5\text{Se}^+$   $[\text{M}+\text{Ag}]^+$ : 432.9678. Found: 432.9730.

### 3.4. Synthesis of 16a,19a-trans-Tetradecahydroselenopheno[3,4-b][1,4,7,10,13,16]hexaoxacyclooctadecine (3)

DHS-crown-6 (3) was obtained from DHS (112 mg, 0.67 mmol) and pentaethyleneglycol ditosylate (500 mg, 1.3 eq) as a colorless oil. The crude product was purified by silica gel column chromatography (dichloromethane–methanol 9:1) and GPC. Yield 141 mg (58%). Spectral for 3:  $^1\text{H}$  NMR ( $\text{CDCl}_3$ )  $\delta$  4.27 (m, 2H), 3.76–3.61 (m, 20H), 3.05 (dd,  $J = 4.0$  and  $10.0$  Hz, 2H), 2.88 (br dd,  $J = 3.0$  and  $9.5$  Hz, 2H).  $^{13}\text{C}$  NMR ( $\text{CDCl}_3$ )  $\delta$  85.4, 71.1, 70.7, 68.9, 24.6.  $^{77}\text{Se}$  NMR ( $\text{CDCl}_3$ )  $\delta$  90.4. HRMS (MALDI-TOF-MS)  $m/z$  calcd for  $\text{C}_{14}\text{H}_{26}\text{AgO}_6\text{Se}^+$   $[\text{M}+\text{Ag}]^+$ : 476.9940. Found: 476.9982.

### 3.5. Synthesis of 19a,22a-Trans-hexadecahydroselenopheno[3,4-b][1,4,7,10,13,16,19]heptaoxacyclohencosine (4)

DHS-crown-7 (4) was obtained from DHS (109 mg, 0.65 mmol) and hexaethyleneglycol ditosylate (531 mg, 1.3 eq) as a slightly yellow oil. The crude product was purified by silica gel column chromatography (dichloromethane–methanol 9:1) and GPC. Yield 158 mg (59%). Spectral for 4:  $^1\text{H}$  NMR ( $\text{CDCl}_3$ )  $\delta$  4.15 (m, 2H), 3.64–3.60 (m, 24H), 3.00 (dd,  $J = 4.0$  and  $10.0$  Hz, 2H), 2.85 (dd,  $J = 4.0$  and  $10.0$  Hz, 2H).  $^{13}\text{C}$  NMR ( $\text{CDCl}_3$ )  $\delta$  85.4, 71.0, 70.9, 70.8, 70.8, 70.7, 69.1, 24.1.  $^{77}\text{Se}$  NMR ( $\text{CDCl}_3$ )  $\delta$  88.3. HRMS (MALDI-TOF-MS)  $m/z$  calcd for  $\text{C}_{16}\text{H}_{30}\text{AgO}_7\text{Se}^+$   $[\text{M}+\text{Ag}]^+$ : 521.0202. Found: 521.0330.

### 3.6. Complex Preparation

The prepared DHS-crowns (1–4) were separately dissolved in methanol. To each solution, an alkali metal salt (1 eq), i.e., KI or NaBr, was added, and the mixture was left still at room temperature to allow for the slow vaporization of the solvent. Crystals were grown and collected by filtration.

### 3.7. X-ray Analysis

Single-crystal X-ray diffraction data for DHS-crown-4 (1) and DHS-crown-4·0.5KI·H<sub>2</sub>O (5) were recorded on a Rayonix-MX225-HS CCD area detector coupled with a synchrotron radiation ( $\lambda = 0.70000 \text{ \AA}$ ) and processed with HKL3000 [35] at 2D beamline in Pohang Accelerator Laboratory (PAL, Pohang, South Korea). Diffraction data for DHS-crown-4·0.5NaBr·2H<sub>2</sub>O (6), DHS-crown-5·0.5KI (7) and DHS-crown-6·KI (8) were measured with a Rigaku XtaLAB PRO P200 diffractometer using graphite monochromated Mo K $\alpha$  radiation or multi-layer mirror monochromated Cu K $\alpha$  radiation. The collected data were processed with CrysAlisPro (Rigaku Oxford Diffraction: Tokyo, Japan, 2015) or CrystalClear (Rigaku Corporation: Tokyo, Japan, 2015). The initial structures were solved by SHELXT (Version 2018/2) [36], except for DHS-crown-6·KI (8). The initial structure of DHS-crown-6·KI (8) was solved by SHELXS (Version 2013/1) [37]. The structure refinement was carried out by the full-matrix least-squares method on  $F^2$  using SHELXL (Version 2018/3) [37]. The CIF files for these compounds were deposited on CCDC (2248791–2248795).

### 3.8. <sup>1</sup>H NMR Titration Study in CD<sub>3</sub>OD

DHS-crown-6 (3) (9.1 mg, 0.025 mmol) was dissolved in CD<sub>3</sub>OD (550  $\mu$ L). The solution was transferred into an NMR test tube, and the <sup>1</sup>H NMR spectrum was recorded. In a different small vial, an alkali metal salt, such as KI, CsCl or RbCl (0.10 mmol, 4 eq), was dissolved in CD<sub>3</sub>OD (200  $\mu$ L). A small portion of D<sub>2</sub>O was added if the salt was imperfectly soluble. To make a solution of KBPh<sub>4</sub>, DMSO-*d*<sub>6</sub> (120  $\mu$ L) was used as the solvent. An aliquot of the solution was added to the solution of 3, and the <sup>1</sup>H NMR spectrum was recorded after standing for more than 30 min. The spectrum measurement was repeated with additions of the aliquots.

### 3.9. Redox Assay for DHS-crown-6 (3)

According to the literature [24], DTT<sup>red</sup> (0.15 mmol) and a catalytic amount of 3 (0.015 mmol) were dissolved in CD<sub>3</sub>OD (1.1 mL) at 25 °C in an NMR test tube. A portion of 30% H<sub>2</sub>O<sub>2</sub> (0.15 mmol), the exact concentration of which was titrated in advance with potassium permanganate, was added to the test tube, and the 500 MHz <sup>1</sup>H NMR spectrum was measured after certain periods of the reaction time. The well separated peaks of DTT<sup>red</sup> and DTT<sup>ox</sup> were integrated to calculate the ratio of the residual DTT<sup>red</sup>. In the assay for the KCl complex, KCl (0.015 mmol) was added with 3. The reproductivity of the results was confirmed by repeating the experiments more than three times.

### 3.10. Theoretical Calculation

DFT calculation was performed using a Gaussian09 rev.B.01 program [38]. The geometry was fully optimized at the B3LYP/6-311+g(2df,p) level in methanol with a polarizable continuum model (PCM). The resulting structures for the two conformers of DHS were characterized as a stationary point with no imaginary vibrational frequency. A summary of the calculation results is provided in the Supplementary Materials.

## 4. Conclusions

We synthesized a series of DHS-crown-*n* (*n* = 4–7) (1–4) and studied the complex formation with various alkali metal salts. According to the X-ray analysis, it was found that DHS-crowns change the conformation of the DHS ring from diaxial to diequatorial by coordination to an alkali metal ion. This conformational change was also confirmed by solution NMR study for DHS-crown-6 (3). In the literature, several crown ether derivatives, in which the crown-ether ring is fused by a five-membered ring system, such as tetrahydrofuran, pyrrolidine, and cyclopetane, have been reported [39–41]. However, the conformational transition of the five-membered ring system induced by the coordination to a guest ion was not reported previously, as per our literature survey. We further demonstrated the application of this interesting phenomenon to the control of the redox catalytic activity in the presence or absence of an alkali metal ion. Although completely turning off the activity

by the addition of an alkali metal ion was not achieved here, this system will be valuable for further investigation for developing redox molecular switches or alkali metal ion sensors.

**Supplementary Materials:** The following supporting information can be downloaded at: <https://www.mdpi.com/article/10.3390/molecules28083607/s1>, Figures S1–S24: NMR and MS spectra; Figure S25: Molecular structures obtained by DFT calculation; Tables S1 and S2: Crystallographic data; Tables S3 and S4: Cartesian coordinates for DHS.

**Author Contributions:** Conceptualization, M.I.; methodology, M.I., H.O. and T.I.; validation, M.I. and T.I.; formal analysis, H.O. and T.I.; investigation, H.O.; writing—original draft preparation, M.I.; writing—review and editing, T.I.; supervision, M.I. All authors have read and agreed to the published version of the manuscript.

**Funding:** This research was funded by JSPS, grant number 22K05466 (M.I.).

**Data Availability Statement:** The data presented in this study are available on request from the corresponding author.

**Acknowledgments:** We thank Matthew Tailby, Takuya Maeda, Toshiyuki Misawa, Fujito Yamaguchi, Shota Arai and Haruki Hasegawa for their assistance with the synthesis and the X-ray analysis. Synchrotron X-ray diffraction measurements were carried out at 2D Beamline, the Pohang Accelerator Laboratory (PAL), supported by Pohang University of Science and Technology (POSTECH). Tatsuhiro Kojima (Osaka University) is acknowledged for his helpful advice on the structural analysis of DHS-crown-6·KI (8).

**Conflicts of Interest:** The authors declare no conflict of interest.

## References

1. Panda, A. Chemistry of Seleno Macrocycles. *Coord. Chem. Rev.* **2009**, *253*, 1056–1098. [CrossRef]
2. Liu, Z.; Nalluri, S.K.M.; Fraser Stoddart, J. Surveying Macrocyclic Chemistry: From Flexible Crown Ethers to Rigid Cyclophanes. *Chem. Soc. Rev.* **2017**, *46*, 2459–2478. [CrossRef]
3. Ren, Y.; Jamagne, R.; Tetlow, D.J.; Leigh, D.A. A Tape-Reading Molecular Ratchet. *Nature* **2022**, *612*, 78–82. [CrossRef]
4. Pfeifer, L.; Crespi, S.; van der Meulen, P.; Kemmink, J.; Scheek, R.M.; Hilbers, M.F.; Buma, W.J.; Feringa, B.L. Controlling Forward and Backward Rotary Molecular Motion on Demand. *Nat. Commun.* **2022**, *13*, 2124. [CrossRef]
5. Ariga, K. Molecular Machines and Microrobots: Nanoarchitectonics Developments and On-Water Performances. *Micromachines* **2022**, *14*, 25. [CrossRef]
6. Li, J.; Yim, D.; Jang, W.D.; Yoon, J. Recent Progress in the Design and Applications of Fluorescence Probes Containing Crown Ethers. *Chem. Soc. Rev.* **2017**, *46*, 2437–2458. [CrossRef]
7. Chowdhury, S.; Rooj, B.; Dutta, A.; Mandal, U. Review on Recent Advances in Metal Ions Sensing Using Different Fluorescent Probes. *J. Fluoresc.* **2018**, *28*, 999–1021. [CrossRef]
8. Bruemmer, K.J.; Crossley, S.W.M.; Chang, C.J. Activity-Based Sensing: A Synthetic Methods Approach for Selective Molecular Imaging and Beyond. *Angew. Chem. Int. Ed.* **2020**, *59*, 13734–13762. [CrossRef] [PubMed]
9. Krämer, J.; Kang, R.; Grimm, L.M.; De Cola, L.; Picchetti, P.; Biedermann, F. Molecular Probes, Chemosensors, and Nanosensors for Optical Detection of Biorelevant Molecules and Ions in Aqueous Media and Biofluids. *Chem. Rev.* **2022**, *122*, 3459–3636. [CrossRef] [PubMed]
10. Barton, A.J.; Genge, A.R.J.; Hill, N.J.; Levason, W.; Orchard, S.D.; Patel, B.; Reid, G.; Ward, A.J. Recent Developments in Thio-, Seleno-, and Telluro-Ether Ligand Chemistry. *Heteroat. Chem.* **2002**, *13*, 550–560. [CrossRef]
11. Laitinen, R.S.; Oilunkaniemi, R.; Weigand, W. Structure, Bonding, and Ligand Chemistry of Macrocyclic Seleno- and Telluroethers. In *Chalcogen Chemistry: Fundamentals and Applications*; Lippolis, V., Santi, C., Lenardao, E.J., Braga, A.L., Eds.; Royal Society of Chemistry: Croydon, UK, 2023; pp. 550–566. ISBN 978-1-83916-422-4.
12. Tsuchiya, T.; Kurihara, H.; Sato, K.; Wakahara, T.; Akasaka, T.; Shimizu, T.; Kamigata, N.; Mizorogi, N.; Nagase, S. Supramolecular Complexes of La@C82 with Unsaturated Thiocrown Ethers. *Chem. Commun.* **2006**, *14*, 3585–3587. [CrossRef] [PubMed]
13. Ferrier, M.G.; Kmak, K.N.; Kerlin, W.M.; Valdez, C.A.; Despotopoulos, J.D. Transactinide Studies with Sulfur Macrocyclic Extractant Using Mercury. *J. Radioanal. Nucl. Chem.* **2020**, *326*, 215–222. [CrossRef]
14. Sabah, K.J.; Sead, F.F.; Mohammed, H.J.; Abedul-Hussien, I.H. Novel Polymer Crafted Sugar Thiocrown Ether and Its Applications in Recovery of Metal Ions. *Carbohydr. Res.* **2020**, *495*, 108057. [CrossRef] [PubMed]
15. Wang, J.; Wang, H.H.; Li, J.Z.; Yao, Z.X.; Cheng, X.; Yu, D.N.; Yan, X.W.; Wang, W.; Liu, K.G. 1,3,5-Trithian Mediated Formation of Two New Tetranuclear Silver-Alkynyl Clusters and Investigation of Their Optical Features. *J. Clust. Sci.* **2022**, *33*, 2363–2368. [CrossRef]
16. Tomoda, S.; Iwaoka, M. Synthesis and Structures of Host Molecules Containing an Se-Se Bond. Intramolecular Hypervalent Nature of Selenium Atoms in the Crystal State. *J. Chem. Soc. Chem. Commun.* **1990**, 231–233. [CrossRef]

17. Raju, S.; Butcher, R.J.; Singh, H.B. Isolation and Structure of an 18-Membered Macrocyclic Containing Two Diselenide Linkages and Its Precursor. *Acta Crystallogr. C Struct. Chem.* **2019**, *75*, 336–341. [[CrossRef](#)]
18. Jayasree, E.G.; Sukumar, C. Integrating Redox-Response in Crown Ethers by Disulfide Incorporation: A Computational Approach. *Struct. Chem.* **2021**, *32*, 1833–1842. [[CrossRef](#)]
19. Hirabayashi, K.; Nakashizuka, M.; Shimizu, T. Synthesis, Structure, and Properties of Unsaturated Thiocrown Ethers Possessing Sulfonium Groups. *Chem. Asian J.* **2022**, *17*, e202101329. [[CrossRef](#)] [[PubMed](#)]
20. Shang, J.; Li, B.; Shen, X.; Pan, T.; Cui, Z.; Wang, Y.; Ge, Y.; Qi, Z. Selenacrown Macrocyclic in Aqueous Medium: Synthesis, Redox-Responsive Self-Assembly, and Enhanced Disulfide Formation Reaction. *J. Org. Chem.* **2021**, *86*, 1430–1436. [[CrossRef](#)] [[PubMed](#)]
21. Li, B.; Xu, Q.; Shen, X.; Pan, T.; Shang, J.; Ge, Y.; Qi, Z. Atom-Economic Macrocyclic Amphiphile Based on Guanidinium-Functionalized Selenacrown Ether Acting as Redox-Responsive Nanozyme. *Chin. Chem. Lett.* **2023**, *34*, 108015. [[CrossRef](#)]
22. Rodewald, M.; Rautiainen, J.M.; Nisch, T.; Görls, H.; Oilunkaniemi, R.; Weigand, W.; Laitinen, R.S. Chalcogen-Bonding Interactions in Telluroether Heterocycles [Te(CH<sub>2</sub>)<sub>m</sub>] (N = 1–4; M = 3–7). *Chem. A Eur. J.* **2020**, *26*, 13806–13818. [[CrossRef](#)] [[PubMed](#)]
23. Iwaoka, M.; Kumakura, F. Applications of Water-Soluble Selenides and Selenoxides to Protein Chemistry. *Phosphorus Sulfur Silicon Relat. Elem.* **2008**, *183*, 1009–1017. [[CrossRef](#)]
24. Kumakura, F.; Mishra, B.; Priyadarsini, K.I.; Iwaoka, M. A Water-Soluble Cyclic Selenide with Enhanced Glutathione Peroxidase-like Catalytic Activities. *Eur. J. Org. Chem.* **2010**, *2010*, 440–445. [[CrossRef](#)]
25. Chakraborty, S.; Yadav, S.K.; Subramanian, M.; Priyadarsini, K.I.; Iwaoka, M.; Chattopadhyay, S. DL-Trans-3,4-Dihydroxy-1-Selenolane (DHSred) Accelerates Healing of Indomethacin-Induced Stomach Ulceration in Mice. *Free Radic Res.* **2012**, *46*, 1378–1386. [[CrossRef](#)]
26. Chakraborty, S.; Yadav, S.K.; Subramanian, M.; Iwaoka, M.; Chattopadhyay, S. DL-Trans-3,4-Dihydroxy-1-Selenolane (DHSred) Heals Indomethacin-Mediated Gastric Ulcer in Mice by Modulating Arginine Metabolism. *Biochim. Biophys. Acta Gen. Subj.* **2014**, *1840*, 3385–3392. [[CrossRef](#)]
27. Iwaoka, M.; Katakura, A.; Mishima, J.; Ishihara, Y.; Kunwar, A.; Priyadarsini, K.I. Mimicking the Lipid Peroxidation Inhibitory Activity of Phospholipid Hydroperoxide Glutathione Peroxidase (GPx4) by Using Fatty Acid Conjugates of a Water-Soluble Selenolane. *Molecules* **2015**, *20*, 12364–12375. [[CrossRef](#)] [[PubMed](#)]
28. Iwaoka, M.; Sano, N.; Lin, Y.Y.; Katakura, A.; Noguchi, M.; Takahashi, K.; Kumakura, F.; Arai, K.; Singh, B.G.; Kunwar, A.; et al. Fatty Acid Conjugates of Water-Soluble (±)-Trans-Selenolane-3,4-Diol: Effects of Alkyl Chain Length on the Antioxidant Capacity. *ChemBioChem* **2015**, *16*, 1226–1234. [[CrossRef](#)]
29. Verma, P.; Kunwar, A.; Arai, K.; Iwaoka, M.; Priyadarsini, K.I. Mechanism of Radioprotection by Dihydroxy-1-Selenolane (DHS): Effect of Fatty Acid Conjugation and Role of Glutathione Peroxidase (GPx). *Biochimie* **2018**, *144*, 122–133. [[CrossRef](#)]
30. Iwaoka, M.; Takahashi, T.; Tomoda, S. Syntheses and Structural Characterization of Water-Soluble Selenium Reagents for the Redox Control of Protein Disulfide Bonds. *Heteroat. Chem.* **2001**, *12*, 293–299. [[CrossRef](#)]
31. Phadnis, P.P.; Wadawale, A.; Priyadarsini, K.I.; Jain, V.K.; Iwaoka, M. Synthesis, Characterization, and Structure of Trans-3,4-Dihydroxy-1-Selenolane {DHS(OH)<sub>2</sub>} Substituted Derivatives. *Tetrahedron. Lett.* **2015**, *56*, 2293–2296. [[CrossRef](#)]
32. Iwaoka, M.; Hiyoshi, Y.; Arai, S.; Ito, T. Synthesis of 4-Selenothiofuranose Derivatives via Pummerer-Type Reactions of Trans-3,4-Dioxygenated Tetrahydro-selenophenes Mediated by a Selenonium Intermediate. *ACS Omega* **2021**, *6*, 17621–17634. [[CrossRef](#)] [[PubMed](#)]
33. Arai, K.; Iwaoka, M. Oxidative Protein Folding Using Trans-3,4-Dihydroxyselenolane Oxide. In *Methods in Molecular Biology*; Humana Press Inc.: Torvalds, NJ, USA, 2019; Volume 1967, pp. 229–244.
34. Bouzide, A.; Sauv e, G. Silver(I) Oxide Mediated Highly Selective Monotosylation of Symmetrical Diols. Application to the Synthesis of Polysubstituted Cyclic Ethers. *J. Am. Chem. Soc.* **2002**, *124*, 16. [[CrossRef](#)]
35. Minor, W.; Cymborowski, M.; Otwinowski, Z.; Chruszcz, M. HKL-3000: The Integration of Data Reduction and Structure Solution—from Diffraction Images to an Initial Model in Minutes. *Acta Crystallogr. Sect. D Biol. Crystallogr.* **2006**, *62*, 859–866. [[CrossRef](#)]
36. Sheldrick, G.M. SHELXT—Integrated Space-Group and Crystal-Structure Determination. *Acta Crystallogr. A Found Adv.* **2015**, *71*, 3–8. [[CrossRef](#)]
37. Sheldrick, G.M. A Short History of SHELX. *Acta Crystallogr. A* **2008**, *64*, 112–122. [[CrossRef](#)] [[PubMed](#)]
38. Frisch, M.J.; Trucks, G.W.; Schlegel, H.B.; Scuseria, G.E.; Robb, M.A.; Cheeseman, J.R.; Scalmani, G.; Barone, V.; Mennucci, B.; Petersson, G.A.; et al. *Gaussian 09, Revision B.01 2010*; Gaussian, Inc.: Wallingford, CT, USA, 2010.
39. Rastetter, W.H.; Phillion, D.P. Template-Driven Macrolide Closures. *J. Org. Chem.* **2002**, *46*, 3209–3214. [[CrossRef](#)]
40. Kele, P.; Nagy, K.; Kotschy, A. The Development of Conformational-Dynamics-Based Sensors. *Angew. Chem. Int. Ed.* **2006**, *45*, 2565–2567. [[CrossRef](#)]
41. Coppola, C.; Simeone, L.; Trotta, R.; De Napoli, L.; Randazzo, A.; Montesarchio, D. Synthesis and NMR Characterization of a Novel Crown-Ether Ring-Fused Uridine Analogue. *Tetrahedron* **2010**, *66*, 6769–6774. [[CrossRef](#)]

**Disclaimer/Publisher’s Note:** The statements, opinions and data contained in all publications are solely those of the individual author(s) and contributor(s) and not of MDPI and/or the editor(s). MDPI and/or the editor(s) disclaim responsibility for any injury to people or property resulting from any ideas, methods, instructions or products referred to in the content.